THE JOURNAL OF BIOLOGICAL CHEMISTRY VOL. 286, NO. 49, pp. 42349–42359, December 9, 2011

Hyaluronan Synthase 2 (HAS2) Promotes Breast Cancer Cell Invasion by Suppression of Tissue Metalloproteinase Inhibitor 1 (TIMP-1)*[S]

Received for publication, July 1, 2011, and in revised form, October 12, 2011 Published, JBC Papers in Press, October 20, 2011, DOI 10.1074/jbc.M111.278598

Berit Bernert, Helena Porsch, and Paraskevi Heldin[1]

From the Ludwig Institute for Cancer Research, Biomedical Center, Uppsala University, SE-75124 Uppsala, Sweden

Invasion and metastasis are the primary causes of breast cancer mortality, and increased knowledge about the molecular mechanisms involved in these processes is highly desirable. High levels of hyaluronan in breast tumors have been correlated with poor patient survival. The involvement of hyaluronan in the early invasive phase of a clone of breast cancer cell line MDA-MB-231 that forms bone metastases was studied using an *in vivo*-like basement membrane model. The metastatic to bone tumor cells exhibited a 7-fold higher hyaluronan-synthesizing capacity compared with MDA-MB-231 cells predominately due to an increased expression of hyaluronan synthase 2 (HAS2). We found that knockdown of HAS2 completely suppressed the invasive capability of these cells by the induction of tissue metalloproteinase inhibitor 1 (TIMP-1) and dephosphorylation of focal adhesion kinase. HAS2 knockdown-mediated inhibition of basement membrane remodeling was rescued by HAS2 overexpression, transfection with *TIMP-1* siRNA, or addition of TIMP-1-blocking antibodies. Moreover, knockdown of HAS2 suppressed the EGF-mediated induction of the focal adhesion kinase/PI3K/Akt signaling pathway. Thus, this study provides new insights into a possible mechanism whereby HAS2 enhances breast cancer invasion.

A hallmark of the malignant phenotype is acquisition of an invasive phenotype that allows cancer cells to degrade the basement membrane before they enter the circulation via blood or lymphatic vessels. The basement membrane is a specialized form of the extracellular matrix that underlies epithelial cells and surrounds blood vessels (1). Turnover of the basement membrane and extracellular matrix is regulated by the balance between metalloproteinases (MMPs)[2] and their naturally occurring tissue inhibitors of MMP (TIMPs). Up-regulation of MMPs or lack of TIMPs has been reported to be involved in cancer cell invasion (1–3). However, the relationship between MMPs and TIMPs is complex because both of them can be overexpressed in malignancies and be associated with tumorigenesis (4, 5). The MMP family of proteolytic enzymes consists of >20 secreted or membrane-anchored enzymes. MMP2, MMP7, and MMP9 are secreted as latent precursor forms (pro-MMP2, pro-MMP7, and pro-MMP9) that are activated at the cell surface and cleave collagen type IV, which is the principal structural constituent of the basement membrane. Membrane type 1 (MT1) MMP catalyzes the activation of pro-MMP2, which in turn activates pro-MMP9, propagating basement membrane proteolysis (1, 2, 6, 7). MMPs can localize transiently to the plasma membrane and become activated through their interactions with adhesion molecules, such as CD44 (8–10).

Accumulating evidence has demonstrated that CD44 and its ligand hyaluronan, a core component of the extracellular matrix, contribute to the invasive behavior and progression of multiple cancers. CD44 exists in various isoforms, the standard form (CD44s) and the variant forms (CD44v1–10), all of which can bind hyaluronan (11–14). Increased hyaluronan synthesis and increased expression of CD44 have been observed in aggressive breast cancer cells (15, 16). Hyaluronan-activated CD44 signaling has been shown to enhance oncogenic events induced by growth factors and MMPs, and CD44 can form complexes with growth factor receptors, as well as with MMPs (10, 12, 17–19).

The expression of hyaluronan synthases (HAS1, HAS2, and HAS3) increases during embryonic development, as well as during malignant progression, specifically in nests of cancer cells and at the invading edges of breast carcinomas (20–23). Of the three *HAS* genes, *HAS2* is vital because of its involvement in epithelial-mesenchymal transition during embryonic cardiac cushion morphogenesis (24). Notably, overexpression of HAS2 in the epithelium induces the transition of epithelial cells to a more fibroblastic, migratory phenotype and enhances anchorage-independent growth in soft agar, *i.e.* two of the key properties of cells undergoing malignant transformation (25, 26). Moreover, studies both *in vivo* and *in vitro* have shown that ectopic expression of HAS proteins (and consequently, increased hyaluronan synthesis) promotes tumor progression, angiogenesis, and lymphangiogenesis, as well as recruitment of stromal cells (27–29). In contrast, suppression of HAS2 using antisense inhibition or specific siRNA has been shown to suppress the malignant phenotype of breast cancer cells (30, 31). Growth factors, such as PDGF-BB and TGF-β (32–34), as well as tumor promoting agents (phorbol 12-myristate 13-acetate) (32) and glucocorticoids (33, 35), modulate expression of the *HAS* genes, especially the HAS2 isoform. Furthermore, hyalu-

* The work was supported by grants from the Swedish Cancer Society, the Mizutani Foundation for Glycoscience, and the Agnes and Mac Rudbergs Foundation (Uppsala University).

[S] The on-line version of this article (available at http://www.jbc.org) contains supplemental Fig. S1 and Table S1.

[1] To whom correspondence should be addressed: Ludwig Inst. for Cancer Research, Biomedical Center, Uppsala University, Box 595, SE-75124 Uppsala, Sweden. Tel.: 46-18-160414; Fax: 46-18-160420; E-mail: evi.heldin@licr.uu.se.

[2] The abbreviations used are: MMP, metalloproteinase; TIMP, tissue inhibitor of MMP; MT1, membrane type 1; HAS, hyaluronan synthase; FAK, focal adhesion kinase.

ronan levels are modulated by the supply of UDP-sugar substrates that are produced during glycolysis (36). Notably, aberrant hyaluronan production seen in hyperglycemia has been associated with higher *HAS2* mRNA expression (37, 38). Hyaluronan is degraded by hyaluronidases, the most important being HYAL1 and HYAL2 (39).

In this study, we explored the possibility that hyaluronan plays an important role during the initial steps of breast cancer invasion through the basement membrane. We compared the biological properties of wild-type MDA-MB-231 breast cancer cells with those of a clone of this line that forms bone metastases (MDA-MB-231-BM) with regard to hyaluronan-synthesizing capacity, CD44 expression, and interference of MMPs. Our data indicate that the abundant expression of HAS2 by MDA-MB-231-BM cells confers an invasive phenotype by suppression of TIMP-1 expression, presumably increasing MMP activity and consequently basement membrane degradation.

MATERIALS AND METHODS

Cell Culture—The human breast cancer cell line MDA-MB-231 (expressing low progesterone and estrogen receptor levels) (40) was kindly provided by Professor J. Bergh (Karolinska Institute, Stockholm, Sweden), and the clone of this cell line that forms bone metastases (called MDA-MB-231-BM in this study) (41) was kindly provided by professor P. ten Dijke (University of Leiden, Leiden, The Netherlands). Breast cancer cells were routinely maintained in DMEM (Sigma) containing 10% FBS (HyClone).

Creation of MDA-MB-231-BM Cell Lines with HAS2 Stably Knocked Down—To knock down HAS2, two target sequences (NM_005328.1-1880s1c1 and NM_005328.1-916s1c1; designated C2 and C4, respectively) were chosen from the human MISSION® shRNA bacterial glycerol stocks containing pLKO.1-puro_shRNA HAS2 (NM_005328; Sigma). As a control, a non-target shRNA vector (Sigma SHC002) was used. After transfection, MDA-MB-231-BM cells were propagated in selection medium containing puromycin. The degree of HAS2 knockdown in each one of the single cell-derived clones was determined by real-time RT-PCR.

Pericellular and Secreted Hyaluronan—The hyaluronan-containing pericellular matrices around MDA-MB-231 and MDA-MB-231-BM cells with HAS2 knocked down or not were visualized using a particle exclusion assay (42). The hyaluronan content in conditioned media was quantified at different time intervals using a competitive binding assay (43).

RNA Isolation and Real-time RT-PCR Assays—Total RNAs were extracted using the RNeasy mini kit (Qiagen) according to the manufacturer's instructions. Each of the total RNAs was reverse-transcribed to cDNA using the iScript cDNA synthesis kit (Bio-Rad), and real-time PCR was carried out using iQ™ SYBR® Green Supermix (Bio-Rad) according to the manufacturer's protocol. The expression level of each target was normalized to the endogenous reference gene GAPDH, calculated as $2^{-\Delta Ct} \times 100$; $\Delta C_t = C_t$(sample mRNA) $- C_t$(GAPDH mRNA). The specific primers used were designed based on cDNA sequences deposited in the GenBank™ Data Bank and are depicted in supplemental Table S1.

Cell Proliferation—Differences in the proliferative capacity between MDA-MB-231 and MDA-MB-231-BM cells with or without knockdown of HAS2 were examined by counting cell numbers using a particle Coulter counter (Beckman) after detachment with trypsin/EDTA.

Examination of Cell Invasion Using an in Vivo-like Three-dimensional Assay—An *in vitro* three-dimensional invasion assay that simulates the *in vivo* situation was used to monitor cell invasion. Cells suspended in a 1:1 (v/v) mixture of DMEM/F-12 medium supplemented with 5% FBS were embedded into 100-mm^3 Matrigel (growth factor-reduced; BD Biosciences) at a density of 1.5×10^5 cells/well in a 48-well plate. Following gelation, 300 μl of culture medium was added, and the cells were incubated for 24 h. In some of the experiments, Matrigel-embedded MDA-MB-231-BM cells with HAS2 knocked down or not were grown overnight after transient transfection with 2 μg of either pcDNA3-FLAG-mock or pcDNA3-HAS2-FLAG vector using FuGENE HD transfection reagent (5:2 ratio; Roche Applied Science) according to the manufacturer's protocol. The constitutive cellular expression of TIMP-1 was either transiently silenced using ON-TARGET*plus* SMARTpool human TIMP-1 (NM_003254; Dharmacon) using SiLentFect transfection reagent (Bio-Rad) or enhanced by transfection with 0.5 μg of pCMV6-XL5-TIMP-1 (OriGene) using Lipofectamine according to the manufacturer's instructions. As controls, ON-TARGET*plus* non-targeting reagent and mock pCMV6-XL5 vector were used, respectively. The cellular morphology in Matrigel was determined in the absence or presence of blocking polyclonal antibodies against TIMP-1 (Abcam ab77847), as well as in the presence of 5 ng/ml human recombinant TIMP-1 (Calbiochem) or PBS, by phase-contrast microscopy, and cell viability was determined using annexin V (Invitrogen) staining and fluorescence/phase-contrast microscopy (Zeiss Axiovert).

To harvest the cells, the Matrigel was digested with 100 μl of Dispase (50 units/ml; BD Biosciences) in PBS at 37 °C for 45 min, followed by Dispase inactivation using 10 mM EDTA in PBS. The cells were then washed by centrifugation, and cell extracts were further examined by microarray analysis, real-time RT-PCR, or immunoblotting.

Immunoblotting—Cells embedded in Matrigel were harvested and lysed in ice-cold 20 mM Tris buffer (pH 7.9) containing 137 mM NaCl, 5 mM EDTA, 0.5% Triton X-100, and protease inhibitors for 30 min at 4 °C; sheared through a 20-gauge needle; reincubated on ice for another 30 min; and centrifuged at 13,000 rpm for 15 min at 4 °C. Protein concentration in the supernatants was determined using the BCA kit (Pierce). The proteins were separated by SDS-PAGE using a 10% polyacrylamide gel; transferred to a nitrocellulose membrane; blocked in 5% milk in 20 mM Tris (pH 7.9), 137 mM NaCl, 5 mM EDTA, and 1% Tween (TBS/Tween); and immunoblotted using antibodies against CD44 (Hermes-3, 1 μg/ml; generously provided by Professor S. Jalkanen), β-actin (1:10,000; Sigma), HAS2 (1 μg/ml) (43), phospho-Akt (Ser-473) and Akt (1:1000; Cell Signaling Technology), phospho-ERK and ERK (1:1000; Cell Signaling Technology), phospho-JNK and JNK (1:1000; Cell Signaling Technology), phospho-focal adhesion kinase (FAK; Tyr-397) and FAK (1:1000; BD Biosciences), phospho-Smad2 (44) and Smad2 (1:2000; Cell Signaling Technology), and MMP2,

MMP7, MMP9, and MT1-MMP (1:1000; Abcam). Following washings with TBS/Tween, the membranes were incubated with HRP-conjugated secondary antibodies, and immunocomplexes were detected by chemiluminescence and quantified using a scanner and associated software.

Motility and Matrigel Invasion Assay—The migration capacities of MDA-MB-231-BM cells with HAS2 knocked down or not were evaluated using a BD BioCoat control insert Transwell chamber (24-well plate, 8 μm; BD Biosciences) and a cell culture wound assay (31). The wound closure was followed up to 72 h using a Zeiss Axiovert inverted phase-contrast microscope and quantified using ImageJ software. The invasive properties of the cells were quantified in a BD BioCoat growth factor-reduced Matrigel invasion chamber (24-well plate, 8 μm; BD Biosciences) according to the manufacturer's instructions.

Gelatin Zymography—Cells were seeded on Matrigel as described above, and the 24-h conditioned media were separated by SDS electrophoresis using a 10% polyacrylamide gel containing 1 mg/ml gelatin. Briefly, the gel was washed with 2.5% Triton X-100 for 2 h and incubated overnight at 37 °C in MMP activation buffer (10 mM $CaCl_2$, 150 mM NaCl, and 50 mM Tris (pH 7.5)) to allow MMPs to degrade the gelatin (45). The gel was then stained for 4 h in a solution containing 0.2% Coomassie Blue, 7.5% acetic acid, and 50% ethanol at room temperature, followed by destaining in 5% methanol for another 4 h. MMP activity was seen as clear areas in the gel.

cDNA Microarray Analysis—The Oligo GEArray® human extracellular matrix and adhesion molecules microarray kit (SABiosciences) was used to profile the expression of 113 genes possessing key roles in extracellular matrix remodeling and cell adhesion. In brief, MDA-MB-231-BM cells with HAS2 knocked down or not were harvested after overnight growth in Matrigel, after which RNA was extracted, reverse-transcribed, and labeled with biotin-16-UTP (Roche Applied Science). The resulting cRNA was purified, hybridized, and subjected to chemiluminescence detection. Images taken with a CCD camera (Bio-Rad) were analyzed using online GEASuite software (SABiosciences). Genes with a change in expression of >2-fold were considered to be up-regulated, whereas genes exhibiting a decreased expression of <0.5-fold were considered to be down-regulated.

Immunostaining Assay—Cells were transfected for 48 h with 10 nM *FAK* siRNA (ON-TARGET*plus* SMARTpool human PTK2; NM_005607; Dharmacon), *TIMP-1* siRNA, or a scrambled siRNA control and seeded (15,000 cells/well) in 8-well chamber slides. The cells were then starved in 0.1% FBS for 24 h, fixed in 3% paraformaldehyde for 10 min, permeabilized with 0.2% Triton X-100, and blocked in 20% goat serum. They were stained with anti-total FAK (1 μg/ml), anti-TIMP-1 (2 μg/ml; Millipore), or anti-HAS2 (1:500; anti-CGR) (43) antibody in 4% goat serum. Alexa Fluor 568-labeled goat anti-mouse and Alexa Fluor 594-labeled goat anti-rabbit (Molecular Probes) secondary antibodies were used at a concentration of 1:1000 in 1% BSA in PBS. The nuclei were stained with DAPI, and the slides were mounted with ProLong® gold antifade reagent (Invitrogen). Photographs were taken with a Zeiss Axioplan 2 immunofluorescence microscope using Volocity® software.

Annexin Apoptosis Detection Assay—Annexin V was used to detect apoptotic cells (according to the manufacturer's instructions) cultured for 24 h in Matrigel. Briefly, cells were washed with PBS and then with annexin binding buffer (10 mM HEPES, 140 mM NaCl, and 2.5 mM $CaCl_2$ (pH 7.4)). Thereafter, Alexa Fluor 594-labeled annexin V diluted 1:10 in annexin binding buffer was added to the cells, followed by incubation at room temperature for 15 min in the dark. After two washings with annexin binding buffer, microphotographs were taken with a Zeiss Axiovert fluorescence/phase-contrast microscope.

RESULTS

Biological Differences between MDA-MB-231 and MDA-MB-231-BM Cells Correlate with HAS2-induced Hyaluronan Synthesis—Because increased production of hyaluronan and expression of CD44 have been correlated with enhanced malignancy of various tumor cells both *in vitro* and *in vivo* (12, 27, 46), we investigated the expression of hyaluronan and CD44 in MDA-MB-231 cells and MDA-MB-231-BM cells, which form bone metastases. The latter cell line synthesized significantly higher amounts of hyaluronan than MDA-MB-231 cells (Fig. 1*A*), and MDA-MB-231-BM (but not MDA-MB-231) cells were surrounded by hyaluronan-containing pericellular matrices (Fig. 1*B*). To investigate the contribution of hyaluronan-synthesizing and hyaluronan-degrading enzymes to the hyaluronan levels detected in the conditioned media, the mRNA levels of *HAS1*, *HAS2*, and *HAS3*, as well as of *HYAL1* and *HYAL2*, were determined using RT-PCR and correlated with GAPDH mRNA levels. The expression of *HAS1* mRNA was almost undetectable in both cell types, and the mRNA levels of *HAS3* differed only slightly (Fig. 1*C*). Importantly, however, the transcriptional activity of *HAS2* was 77-fold higher in MDA-MB-231-BM cells (2.16% relative to GAPDH) compared with that in MDA-MB-231 cells (0.03% relative to GAPDH). Furthermore, the level of *HYAL1* mRNA was low, whereas that of *HYAL2* mRNA was high in both cell lines (Fig. 1*C*). Thus, the higher hyaluronan-synthesizing capacity of MDA-MB-231-BM cells is most likely due to the increased expression of the *HAS2* gene in these cells. Furthermore, both cell types expressed mRNA for the standard form of CD44 at approximately equal amounts (Fig. 1*C*). They also expressed the variant spliced forms *CD44v3* and *CD44v6* at similar levels, but only at 1 and 0.3% of the *CD44s* isoform, respectively.

Because MMPs form complexes with CD44 molecules and play a pivotal role in the invasive phenotype of cancer cells by promoting the perforation of the basement membrane, we examined the invasive behavior of MDA-MB-231 and MDA-MB-231-BM cells using an *in vivo*-like Matrigel invasion assay (Fig. 1*D*). Following 6 h of incubation in Matrigel, MDA-MB-231 cells remained as single cells, exhibiting an indolent behavior with little invasiveness. In contrast, the MDA-MB-231-BM cells traversed the basement membrane, forming cable-like structures. However, after 24 h of culture, both cell lines had perforated the Matrigel, forming networks (Fig. 1*D*).

Because basement membrane perforation is principally a MMP-mediated process, we compared the expression levels of MMPs in MDA-MB-231 and MDA-MB-231-BM cells by immunoblotting. As shown in Fig. 1*E*, MMP2 and MMP7 were

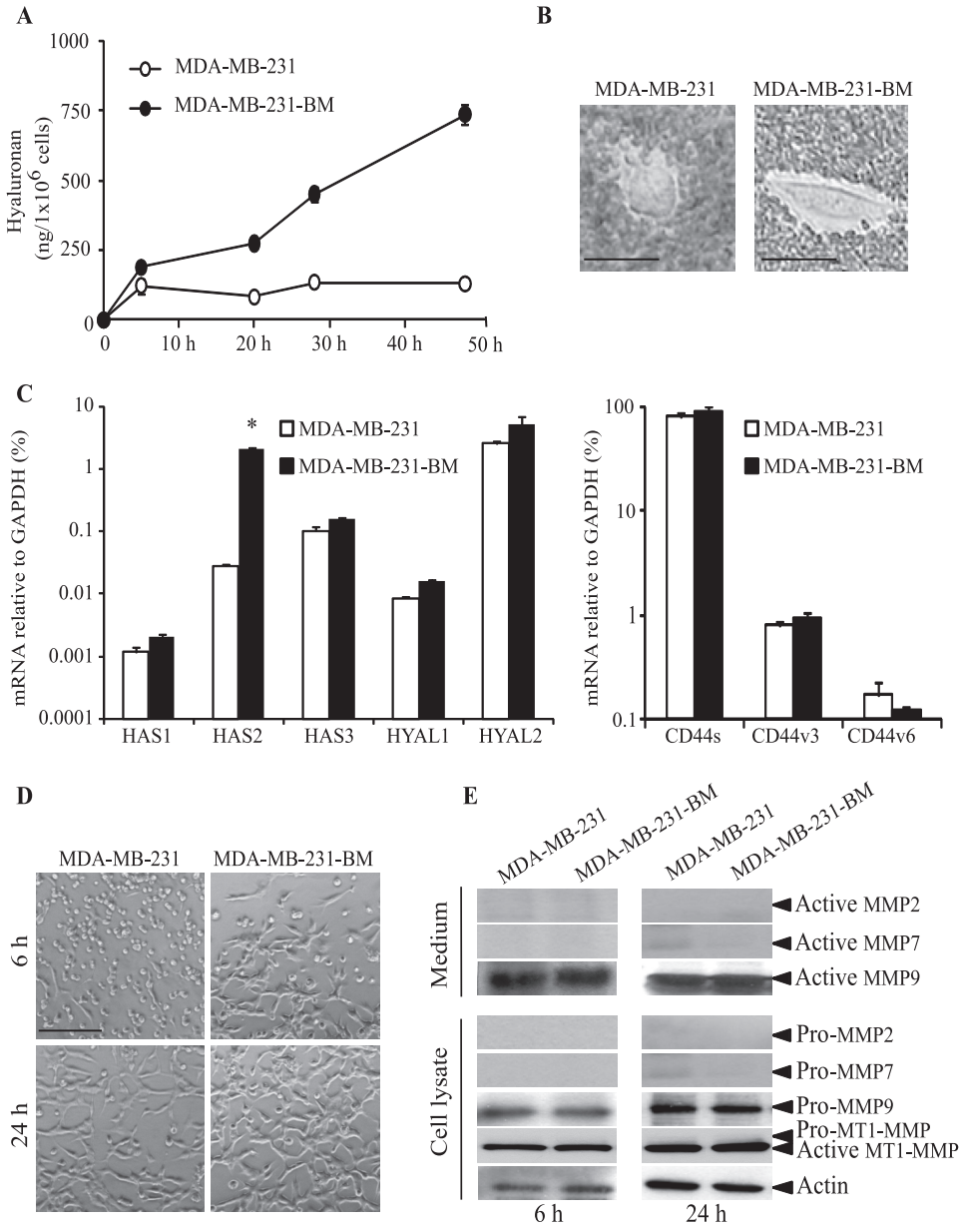

FIGURE 1. **Characterization of MDA-MB-231 and MDA-MB-231-BM cells with regard to hyaluronan production; *HAS*, *HYAL*, and *CD44* mRNA expression; and invasive behavior.** *A*, hyaluronan production. Cells (2×10^5) were seeded in a 6-cm dish and grown for the indicated time periods. Conditioned media were collected, and the hyaluronan amount was determined. The graph shows the average ± S.D. of triplicates. *B*, assembly of pericellular matrices. MDA-MB-231 and MDA-MB-231-BM cells (2×10^4 cells/well) were seeded in 6-well plates, and their hyaluronan coat was determined by a particle exclusion assay after 24 h. Photographs were taken with a Zeiss Axiovert phase-contrast microscope. *Scale bars* = 25 μm. *C*, *HAS*, *HYAL*, and *CD44* mRNA expression. Cells (2×10^5 cells/well) were grown in 12-well plates for 24 h. The expression levels relative to GAPDH of *HAS1*, *HAS2*, *HAS3*, *HYAL1*, *HYAL2*, *CD44s*, *CD44v3*, and *CD44v6* mRNAs were determined by real-time PCR as described under "Materials and Methods." Results are means ± S.D. of triplicate determination. *, $p < 0.05$ (Student's *t* test, significant difference compared with MDA-MB-231 cells). *D*, *in vivo*-like invasion assay. Cells (1.5×10^5 cells/well, 48-well plates) were embedded in 100 μl of growth factor-reduced Matrigel/dish and incubated for 6 or 24 h. Representative pictures were taken with a Zeiss Axiovert phase-contrast microscope. *Scale bar* = 100 μm. *E*, expression of MMP2, MMP7, MMP9, and MT1-MMP proteins. Cell lysates and conditioned media were subjected to SDS-PAGE using 10% polyacrylamide gels, followed by immunoblotting with antisera against MMP2, MMP7, MMP9, MT1-MMP, and actin as described under "Materials and Methods." The data presented are from a representative experiment of two performed with similar results.

barely expressed by any of the cells, whereas MMP9 and MT1-MMP were expressed at high and similar levels by the two cell types.

Stable HAS2 Knockdown Suppresses the Malignant Phenotype of MDA-MB-231-BM Cells—To study whether the high transcriptional activity of *HAS2* in MDA-MB-231-BM cells accounts for their aggressive phenotype, we investigated the consequences of stable knockdown of the *HAS2* gene using specific shRNA. Two different shRNA constructs were used, and several clonal cell lines were derived (supplemental Fig. S1). Clones C2-4 and C4-25 (showing a knockdown efficiency of ~80% at the mRNA level), as well as a control, were chosen for further experiments. Notably, silencing of *HAS2* had no effect on the transcriptional activities of the *HAS1* and *HAS3* genes (Fig. 2*A*). Comparison of the HAS2 protein levels using immunoblotting demonstrated that the HAS2 knockdown clones C2-4 and C4-25 showed efficient knockdown of HAS2 also at the protein level compared with MDA-MB-231-BM control

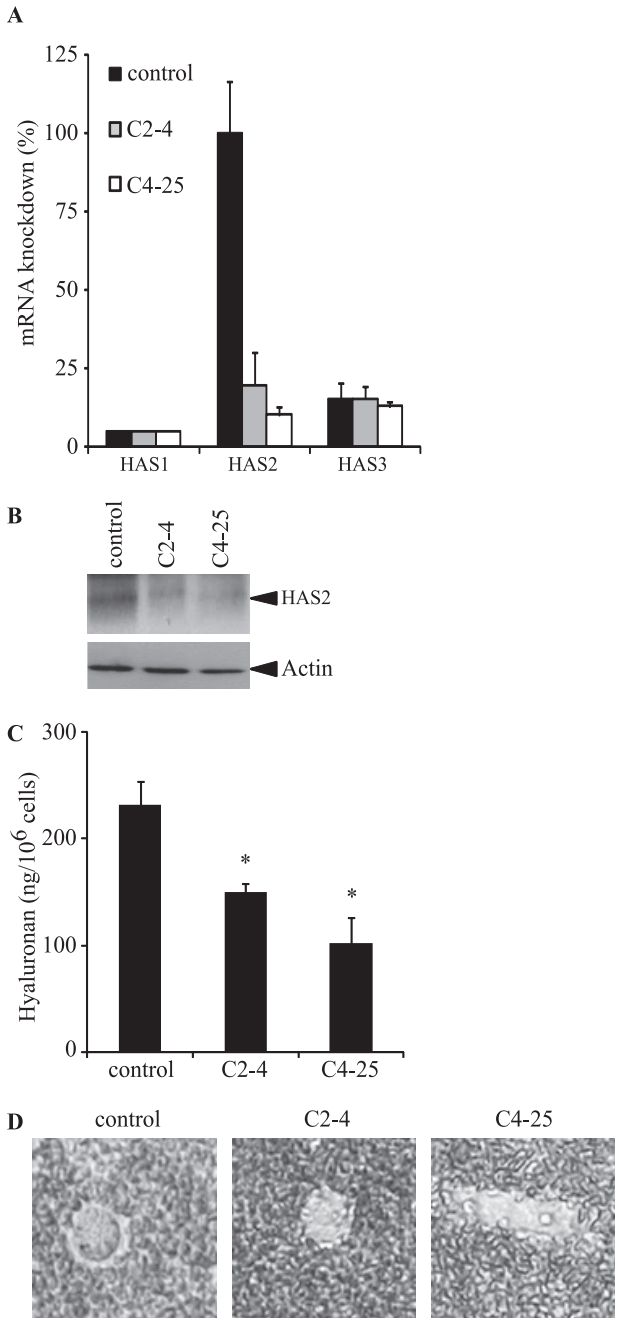

FIGURE 2. **Characterization of MDA-MB-231-BM cells transfected with *HAS2* shRNA.** *A*, effect of *HAS1*, *HAS2*, and *HAS3* mRNAs on expression. Two clones (C2-4 and C4-25) in which HAS2 was silenced by shRNA-expressing vectors, as well as control transfected cells, were subjected to analysis of *HAS1*, *HAS2*, and *HAS3* mRNA expression levels by real-time PCR. Results are means ± S.D. of triplicate determination. *B*, effect of HAS2 protein on expression. Cell lysates were subjected to SDS-PAGE, followed by immunoblotting with antisera against HAS2 (anti-CGR) and actin. *C*, effect on hyaluronan production. The hyaluronan content of 24-h conditioned media was determined in an ELISA-like approach as described under "Materials and Methods." Results are means ± S.D. of triplicate determination. *, $p < 0.05$ (Student's *t* test, significant difference compared with control cells). *D*, effect on pericellular matrices. Hyaluronan-containing pericellular matrices surrounding cells expressing HAS2 or not were determined by a particle exclusion assay after 24 h. Photographs were taken with a Zeiss Axiovert phase-contrast microscope. The data presented are from a representative experiment of two performed with similar results.

cells (Fig. 2*B*). This was also confirmed by immunohistochemical stainings in which HAS2 was visualized all over the cells in patch-like structures. The staining was dramatically decreased in HAS2-deprived cells as expected (data not shown). Notably, HAS2 knockdown clones possessed ~60% of the hyaluronan-synthesizing capacity of HAS2-expressing cells (Fig. 2*C*), suggesting that HAS3 expression by HAS2 knockdown clones C2-4 and C4-25 accounts for part of the total amount of the synthesized hyaluronan; the fact that HAS3 synthesizes shorter hyaluronan chains may explain why the pericellular matrices around C2-4 and C4-25 cells were barely detected compared with control cells (Fig. 2*D*).

There was no effect on the expression levels of CD44s either in the precursor or active forms of MMP9 or MT1-MMP (Fig. 3*A*) in HAS2 knockdown or HAS2-expressing cells. Moreover, gelatin zymography of cell culture media revealed bands with molecular masses of ~20, 70, 90, and 130 kDa, which correspond to the molecular masses of MMP7, MMP2, MMP9, and MMP2 dimers, respectively; there was no difference in the media from cells expressing HAS2 or not. This technique allows the detection of both the active and latent forms of MMPs (47). A striking finding of this study was that HAS2 silencing caused an ~4-fold decrease in the proliferative capacity of MDA-MB-231-BM cells (Fig. 3*B*), indicating that HAS2 expression is important for the proliferative capacity of these cells. Although HAS2 silencing had no effect on CD44 and MMP expression (Fig. 3*A*), which regulates both migration and invasion, we unexpectedly found that it caused an ~60% inhibition of the motility of MDA-MB-231-BM cells measured using a cell culture wounding assay (data not shown). Similarly, using a Transwell chamber assay (BD BioCoat control inserts), the migration ability of HAS2 knockdown cells was ~60% lower compared with HAS2-expressing cells (Fig. 3*C*). Moreover, the involvement of HAS2 in the invasive behavior of these cell types was also studied using Transwell chambers layered with Matrigel matrix. The analysis revealed that the transmigration of clones C2-4 and C4-25, in which HAS2 was knocked down, was ~80% inhibited compared with control shRNA-transfected MDA-MB-231-BM cells (Fig. 3*C*). These findings indicate that HAS2 and, most likely, the endogenous HAS2-synthesized hyaluronan are important in maintaining the aggressive phenotype of breast cancer cells.

To simulate *in vivo* invasiveness, cells were embedded into 100-mm^3 Matrigel. MDA-MB-231-BM cells expressing HAS2 perforated the Matrigel and formed cable-like structures, whereas knockdown of HAS2 led to strikingly rounded cells that were unable to perforate the matrix (Fig. 4). Importantly, the re-expression of HAS2 in these cells switched them back to an invasive phenotype (Fig. 4), showing that the suppressed transmigration of the C2-4 and C4-25 cells was not due to clonal selection. Thus, HAS2 confers an invasive phenotype to MDA-MB-231-BM cells, most likely by inducing a Matrigel-remodeling activity. Notably, the suppression of HAS2 in MDA-MB-231-BM cells did not induce apoptosis because annexin V staining was nearly undetectable (data not shown).

MDA-MB-231-BM Cell-mediated Perforation of Matrigel Is Affected by Regulation of HAS2 and TIMP-1 Activities—To elucidate the molecular mechanisms for the HAS2-dependent

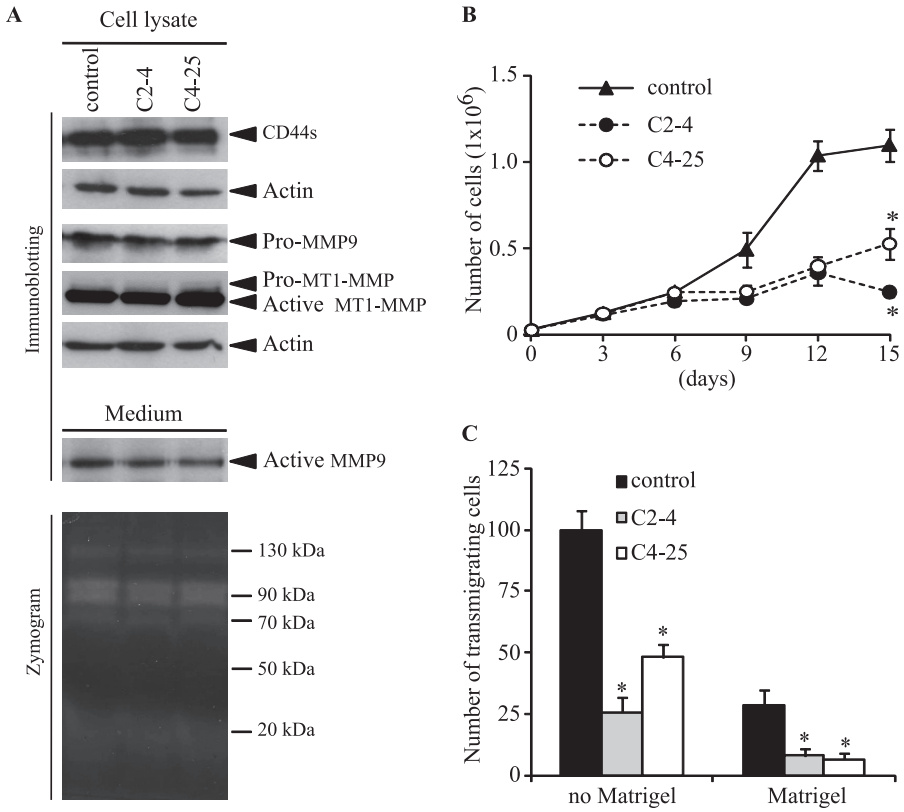

FIGURE 3. **Further characterization of MDA-MB-231-BM cells transfected with *HAS2* shRNA.** *A*, effect of CD44, MMP9, and MT1-MMP proteins and MMP activity on expression. Cell lysates or conditioned media from cells grown on Matrigel were subjected to SDS-PAGE, followed by immunoblotting for CD44, MMP9, and MT1-MMP. MMP activity was determined in by gelatin zymography. Shown is a representative experiment of two separate experiments performed with similar results. *B*, effect on cell proliferation. The cell numbers of control *HAS2* shRNA-expressing, *HAS2* shRNA-expressing C2-4, and *HAS2* shRNA-expressing C4-25 MDA-MB-231-BM cells were measured up to 15 days after seeding. *C*, effect on cell migration and invasion. Unlayered and Matrigel-layered Transwell 24-well units (8-μm pore size) were used for the migration and invasion assays, respectively. In both *B* and *C*, data represent the mean of triplicates from one of two separate experiments. *, $p < 0.05$ (Student's *t* test, significant difference compared with control *HAS2* shRNA-expressing MDA-MB-231-BM cells).

invasion of MDA-MB-231-BM cells, we investigated the possible effects of suppression of HAS2 on components involved in extracellular matrix remodeling or cell adhesion using the Oligo GEArray DNA microarray. Hybridization of labeled cRNA prepared from control cells and the stable HAS2 knockdown clone C4-25 grown embedded in Matrigel for 24 h revealed a number of up-regulated genes in the HAS2-deprived clones (Fig. 5*A*). The most distinctly up-regulated gene was *TIMP-1*. *TIMP-3* expression was much less pronounced. The expression levels of *MMP9* and *MT1-MMP* were not altered (data not shown), whereas the expression of *MMP3* was also increased. Among cell adhesion molecules, SPARC/osteonectin (*SPOCK1*, encoding a plasma membrane proteoglycan containing chondroitin and heparin sulfate chains of unknown function), catenin δ1 (*CTNND1*), and α-integrins (*ITGA2*, *ITGA3*, *ITGA5*, and *ITGA6*) were up-regulated. A number of basement membrane molecules, such as the laminin 5 gene (*LAMA5*) and collagens (*COL6α1* and *COL12α1*), were also increased (Fig. 5*A*).

We then validated the microarray-based findings for some of the genes by real-time RT-PCR. As shown in Fig. 5*B*, we were able to confirm the induction of *TIMP-1* in the HAS2 knockdown C4-25 cells. Furthermore, a slight up-regulation was also seen for *SPOCK1* and *LAMA5*. Furthermore, because the microarray did not include *HYAL1* and *HYAL2*, we investigated also the expression of those genes with real-time RT-PCR; a significant decrease in their expression was observed upon suppression of the *HAS2* gene. Similar RT-PCR-based results were also obtained with HAS2 knockdown C2-4 cells (data not shown). Analyses of the levels of TIMP-1 protein by immunoblotting revealed a marked increase in TIMP-1 levels in HAS2 knockdown clones C2-4 and C4-25 compared with MDA-MB-231 cells expressing HAS2 (Fig. 5*C*).

To investigate whether the effect of HAS2 silencing on the inhibition of invasion is due to the induction of TIMP-1 activity, we transiently transfected the cells with specific siRNA for *TIMP-1* and also grew cells in the presence of TIMP-1-blocking antibodies. In both cases, HAS2-deprived cells regained their invasive ability (Fig. 6*A*), suggesting that the release of active TIMP-1 in the culture media upon HAS2 silencing mediated the inhibitory effect on invasion. We then explored the effects of exogenously added recombinant TIMP-1 and overexpression of TIMP-1 by transfection on the invasive behavior of the cells. A striking reduction in the invasive behavior of HAS2-expressing cells was observed (Fig. 6*B*). Thus, most likely, HAS2 promotes the proinvasive properties of MDA-MB-231-BM cells by suppressing TIMP-1 expression.

Effect of HAS2 Deprivation on Signaling Pathways—To gain insights into the signaling mechanisms that mediate the effect of HAS2 knockdown on TIMP-1 expression, we examined

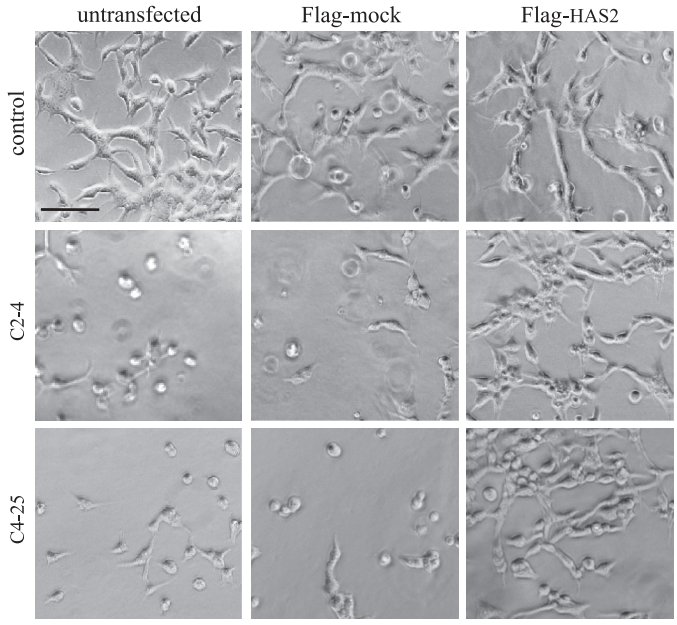

FIGURE 4. **Deprivation of HAS2 inhibits the invasive behavior of MDA-MB-231-BM cells and rescue by HAS2 expression.** Control *HAS2* shRNA-expressing, *HAS2* shRNA-expressing C2-4, and *HAS2* shRNA-expressing C4-25 breast cancer cells were subjected to an *in vivo*-like three-dimensional invasion assay for 24 h as described under "Materials and Methods" prior to or after transfection with FLAG-mock or FLAG-HAS2 constructs. Photographs were taken with a Zeiss Axiovert phase-contrast microscope. *Scale bar* = 100 μm.

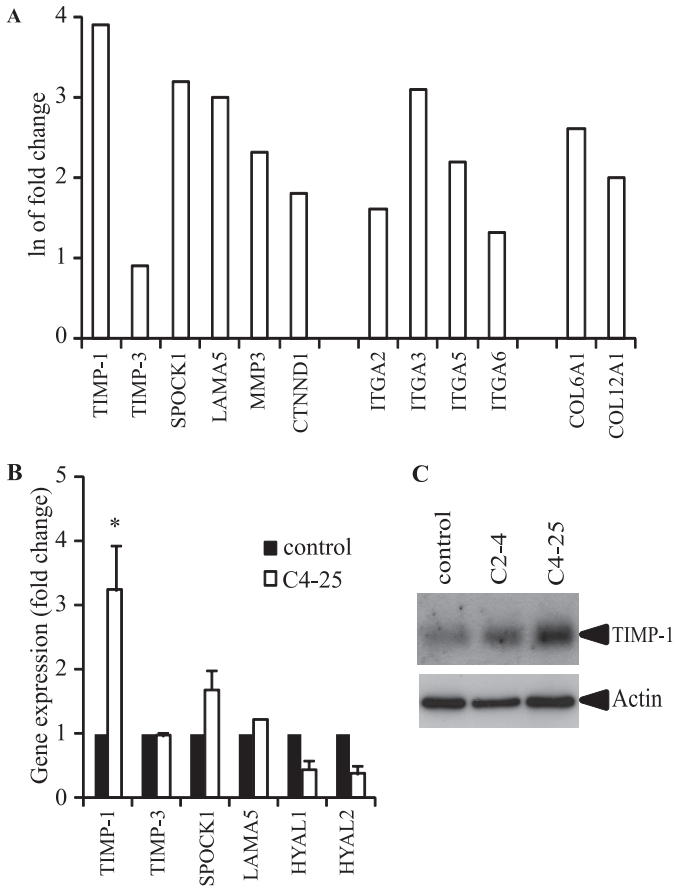

FIGURE 5. **Microarray and real-time RT-PCR gene analyses reveal that HAS2 suppression causes TIMP-1 induction.** Cells were grown embedded in Matrigel for 24 h, after which RNAs were prepared and subjected to microarray (*A*) and RT-PCR (*B*) analyses as described under "Materials and Methods." Displayed are the -fold changes in gene expression in *HAS2* shRNA-expressing C4-25 cells (*open bars*) compared with control *HAS2* shRNA-expressing MDA-MB-231-BM cells (*black bars*). Results show a representative experiment from two separate experiments performed in triplicate. *, $p < 0.05$ (Student's *t* test, statistically significant difference between the two cell types). *C*, immunoblotting. Conditioned media were subjected to immunoblotting for TIMP-1, and correlative amounts of cell lysates were used as loading controls.

changes in the activation state of key signaling molecules. No significant differences were found in the expression and activation levels (phosphorylation state) of ERK, JNK, and Smad2 in MDA-MB-231-BM cells with HAS2 knocked down compared with wild-type MDA-MB-231-BM cells; phospho-Akt was undetectable (Fig. 7*A*). TIMP-1 has been reported to inhibit endothelial cell migration by a mechanism that involves reduced phosphorylation of FAK, which provides a link between the cytoskeleton and extracellular matrix (48). Therefore, we examined the effect of HAS2 deprivation on FAK phosphorylation by immunoblotting. After 24 h of culture in Matrigel, an ~50% decrease in the phosphorylation of FAK was seen in the harvested non-invasive C2-4 and C4-25 MDA-MB-231-BM clones with HAS2 knocked down compared with control cells (Fig. 7*B*).

Interestingly, silencing of *TIMP-1* mRNA increased the phosphorylation of FAK in the C2-4 and C4-25 cell lines to levels similar to those in wild-type MDA-MB-231-BM cells (Fig. 7*B*). Thus, the inhibitory effects of TIMP-1 on cell motility and invasion are reversely correlated with FAK phosphorylation.

Previous studies revealed that HAS2 activity is regulated by EGF (49–51). We investigated whether there is an effect of HAS2 knockdown on EGF signaling with regard to the FAK/PI3K/Akt pathway in our experimental system. We observed a striking reduction in EGF-mediated phosphorylation of Akt in HAS2 knockdown clones (Fig. 7*C*). In addition, siRNA silencing of FAK in MDA-MB-231-BM cells expressing HAS2 inhibited the phosphorylation of Akt (Fig. 7*D*). An inhibitor of PI3K (LY294002) completely abolished EGF-induced phosphorylation of Akt in cells expressing FAK or not, as expected. These results indicate that FAK functions downstream of the activated EGF receptor to mediate activation of the PI3K/Akt signaling pathway and that HAS2 knockdown interferes with that signaling. Furthermore, using immunohistochemistry, we observed that suppression of FAK or TIMP-1 did not interfere with the expression levels of HAS2 (Fig. 8), which places HAS2 upstream of FAK and TIMP-1. Silencing of FAK did not affect TIMP-1 expression (Fig. 8), but knockdown of TIMP-1 rescued the phosphorylation of FAK in HAS2-deprived clones (Fig. 7*B*). These results indicate that TIMP-1 is downstream of HAS2 but upstream of FAK.

DISCUSSION

In this study, we have demonstrated that the invasive MDA-MB-231-BM cells synthesized high amounts of hyaluronan through up-regulation of the *HAS2* gene compared with MDA-MB-231 cells. Suppression of HAS2 decreased the invasive phenotype of MDA-MB-231-BM cells in conjunction with increased expression of TIMP-1; the phenotype was reverted

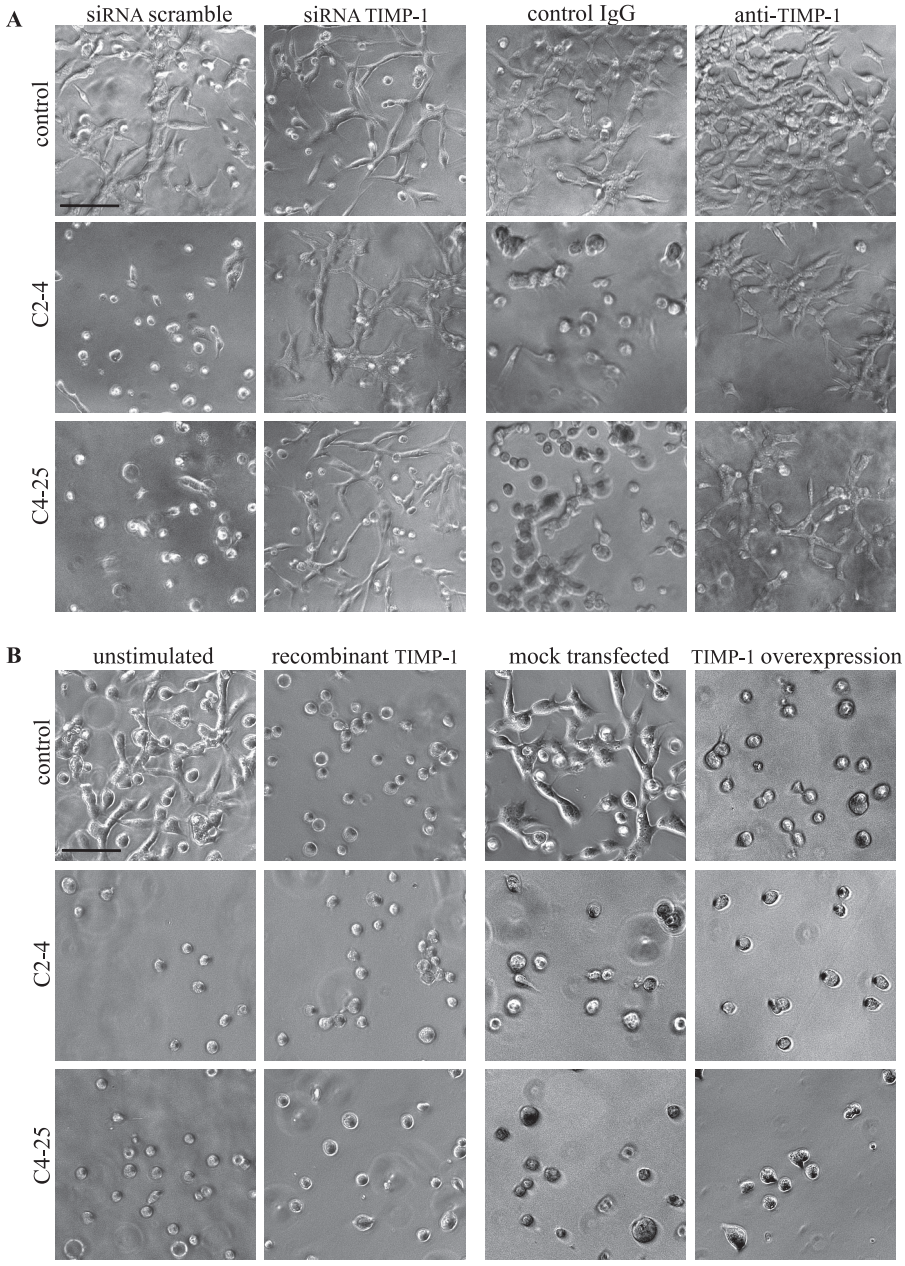

FIGURE 6. *A*, abrogation of HAS2-induced TIMP-1 expression potentiates the invasive potential. MDA-MB-231-BM cells deprived or not of HAS2 were cotransfected with scrambled siRNA or siRNA for *TIMP-1* or treated with control antibodies or blocking antibodies against TIMP-1 during their culturing in *in vivo*-like Matrigel matrix. Photographs were taken after 24 h of culture with a Zeiss Axiovert phase-contrast microscope. *Scale bar* = 100 μm. A representative experiment of three separate experiments performed with similar results is shown. *B*, overexpression of TIMP-1 by transfection or treatment with recombinant TIMP-1 inhibits invasiveness. Control or *HAS2* shRNA knockdown cells were either treated with 5 ng/ml human recombinant TIMP-1 or transfected with pCMV6-XL5-TIMP-1 or mock plasmid, respectively, prior to seeding on Matrigel. Phase-contrast photographs were taken after 24 h. *Scale bar* = 100 μm.

after overexpressing HAS2 (Fig. 4), silencing the *TIMP-1* gene, or addition of TIMP-1-blocking antibodies (Fig. 6*A*).

Our findings are consistent with the observation that coumarin-like 4-methylumbelliferone, an inhibitor of hyaluronan synthesis that exhibits both anti-inflammatory and antitumor properties, increases TIMP-1 expression in aortic smooth muscle cell cultures (52). The reverse correlation between HAS2 and TIMP-1 is most likely a property of hyaluronan endogenously produced by HAS2 because exogenously added hyaluronan in osteoclast cultures (53) and mature hematopoietic cells (54) increases TIMP-1 expression. Our present and previous results (17, 31), as well as those of others (55) support the conclusion that the functional properties of endogenously synthesized hyaluronan cannot always be mimicked by exogenously added hyaluronan.

It is possible that HAS2 has a hyaluronan CD44-independent signaling property because the HAS2 isoform appears to be a trait of breast cancer cells metastasizing to bone, whereas this phenotype is unrelated to the other HASs, hyaluronidases, and CD44 (Fig. 1). Increased understanding of the regulation of the *HAS2* gene and protein in various pathological contexts is desirable. Specific inhibition of the *HAS2* gene and hyaluronan synthesis occurs through glucocorticoids (33, 35) that induce a rapid and sustained decrease in both gene transcription and

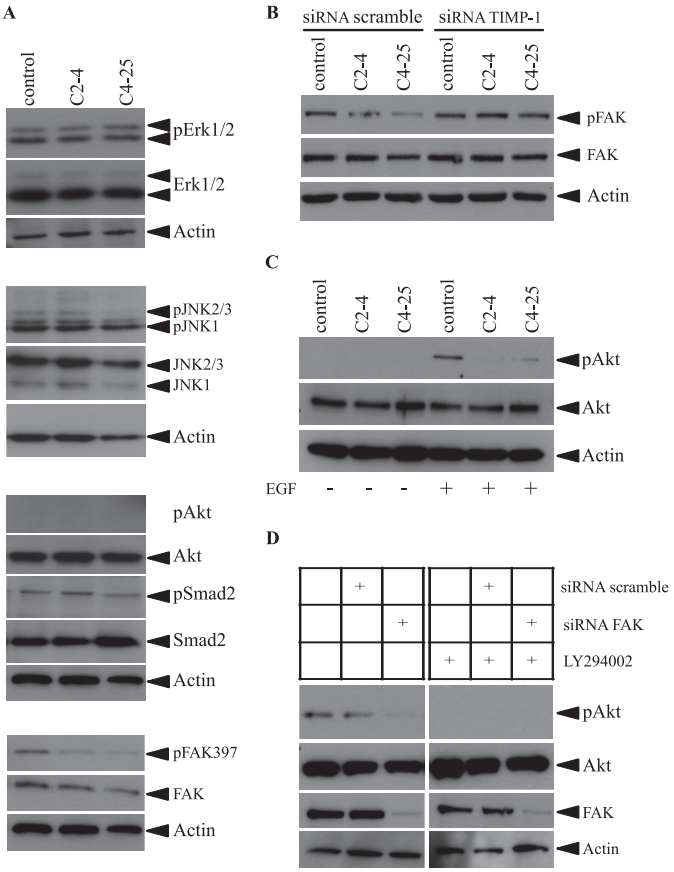

FIGURE 7. **Effect of HAS2 deprivation on signaling pathways.** *A*, activation of signaling molecules. Lysates from control *HAS2* shRNA-expressing or HAS2-deprived C2-4 and C4-25 MDA-MB-231-BM cells cultured under *in vivo*-like conditions were subjected to SDS-PAGE, followed by immunoblotting with antibodies against phospho-ERK, ERK, phospho-JNK, JNK, phospho-Akt, Akt, phospho-Smad2, Smad2, phospho-FAK, and FAK signaling molecules. Actin expression was used as a loading control. *B*, effect of knockdown of TIMP-1 on FAK activation. Immunoblotting was performed on lysate from control *HAS2* shRNA-expressing cells or from HAS2-deprived C2-4 and C4-25 cells that were transiently transfected with siRNA for *TIMP-1*. Immunoblotting was performed with antibodies against phospho-FAK, FAK, and actin. The data presented are from a representative experiment of three performed with similar results. *C*, EGF-mediated activation of Akt. Cells (control or HAS2-deprived clones) were starved overnight, stimulated with 10 ng/ml EGF or Me_2SO, lysed, and subjected to SDS-PAGE, followed by immunoblotting with antibodies against phospho-Akt, Akt, or actin (as a loading control). *D*, effect of FAK suppression on EGF-mediated activation of Akt. HAS2-expressing cells (control *HAS2* shRNA) were transfected with scrambled siRNA or *FAK* siRNA and stimulated with EGF (10 ng/ml) in the absence or presence of the PI3K inhibitor LY294002. Cell lysates were then subjected to immunoblotting with antibodies against phospho-Akt, Akt, FAK, and actin.

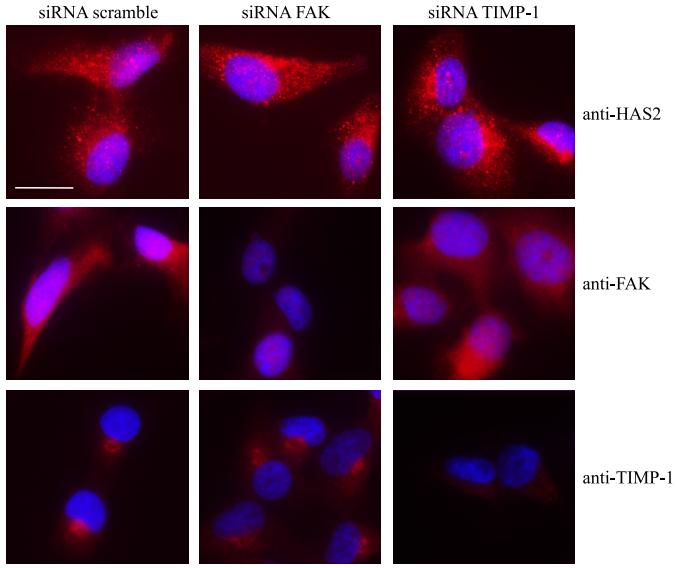

FIGURE 8. **Knockdown of TIMP-1 or FAK does not affect HAS2 expression.** Control *HAS2* shRNA-expressing cells were transfected with scrambled siRNA or siRNA against *TIMP-1* or *FAK*, starved, and subsequently immunostained with antibodies against HAS2 (anti-CGR). *Scale bar* = 11 μm.

HAS2 mRNA stability. Moreover, changes in hyaluronan synthesis can be affected by post-translational modifications of the HAS2 protein through phosphorylation (32) and ubiquitination (56). Accumulating evidence supports the notion that induction of HAS2 often accounts for the increased amount of hyaluronan synthesis seen in many tumors, which correlates with poor outcome. Interestingly, *HAS2* is one of the 0.3% of genes that were up-regulated through tumor-stromal interactions during pancreatic cell invasion (57). Furthermore, *HAS2* has been implicated in chromosomal copy number alterations associated with periodic fever syndrome (58). In addition, *HAS2* chromosomal rearrangements and their deregulated mRNA expression are oncogenic events in lipoblastomas (59) and breast cancer (60). Thus, transcriptional up-regulation of HAS2 might reflect early molecular events in inflammation and cancer. Analysis of the promoter region of the *HAS2* gene indicated transcriptional regulation in response to growth factors, cytokines, and protein kinase C activators through putative Sp1, CREB1, STAT, and NF-κB transcription initiation sites, all of which are fine-balanced to assure hyaluronan production in response to external stimuli (61).

To elucidate the mechanism whereby decreased HAS2 expression and increased TIMP-1 expression could mediate decreased invasiveness, we investigated the activation status of several signaling pathways. No significant differences were noted in cells expressing HAS2 or not with regard to activation of ERK, JNK, and the Smad2 pathway; no activation of Akt was seen in any of the cells. However, we found that HAS2 expression is necessary for EGF-mediated activation of the FAK/PI3K/Akt pathway because this pathway was drastically attenuated upon knockdown of HAS2. Interestingly, knockdown of HAS2 correlated with a decreased activation of FAK, which could be rescued by siRNA-mediated knockdown of TIMP-1.

The TIMP-1-mediated inhibition of matrix remodeling, *e.g.* in conjunction with cancer invasion and inflammation, has been associated with the ability of TIMP-1 to suppress the activities of MMPs. However, TIMP-1 has also been shown to have MMP-independent functions, *i.e.* an anti-apoptotic activity in several cell types, including hematopoietic cells (62) and normal breast epithelial cells via activation of FAK, which binds and activates PI3K, resulting in phosphorylation of Akt and then Bad, known to be crucial for cell survival (63–65). However, there was no difference in the apoptotic rate of cells expressing HAS2 or not as determined by annexin V staining (data not shown). TIMP-1 was shown to inhibit microvascular endothelial cell migration by both MMP-dependent (induction of VE-cadherin) and MMP-independent (inhibition of FAK activity) mechanisms (48). Whether the suppression of MDA-

MB-231-BM cell invasion by TIMP-1 induction following HAS2 knockdown is exerted via MMP-dependent or MMP-independent mechanisms or both remains to be determined. The mechanism whereby TIMP-1 affects FAK phosphorylation remains to be elucidated. However, our finding of a correlation between TIMP-1-induced loss of invasive activity and FAK dephosphorylation is consistent with previous data that demonstrated an important role for FAK in regulation of cell motility (66). Notably, a correlation between down-regulation of FAK and up-regulation of TIMP-1 was recently seen in prostate cancer cells (67).

Bone metastases are common in breast carcinomas. Based on the "seed and soil" theory of Paget (68), bone tissue most likely provides a suitable milieu for breast cancer cells to grow. Hyaluronan and CD44 are abundantly found in breast tumor and bone marrow matrices especially during osteoclastic bone metastases (40, 69). It is possible that high hyaluronan synthesis by breast cancer cells not only plays an important function in determining their early invasive phenotype but could also promote interactions with CD44-expressing cells in the bone tissue microenvironment and create a physiological "niche" in which breast cancer cells thrive.

An increased understanding of the regulation of the *HAS2* gene and protein in various pathological contexts is desirable. Specific inhibition of the *HAS2* gene and hyaluronan synthesis occurs through glucocorticoids (33, 35), which induce a rapid and sustained decrease in both gene transcription and *HAS2* mRNA stability. Moreover, changes in hyaluronan synthesis can be affected by post-translational modifications of HAS2 protein through phosphorylation (32) and ubiquitination (56). In addition to our study, these previous studies provide a rationale for inhibition of hyaluronan synthesis in tumor treatment.

Acknowledgments—We thank C.-H. Heldin for support and constructive criticism of this work and Aino Ruusala for help with the Transwell assay.

REFERENCES

1. Kalluri, R. (2003) *Nat. Rev. Cancer* **3,** 422–433
2. Hotary, K., Li, X. Y., Allen, E., Stevens, S. L., and Weiss, S. J. (2006) *Genes Dev.* **20,** 2673–2686
3. Srivastava, A., Pastor-Pareja, J. C., Igaki, T., Pagliarini, R., and Xu, T. (2007) *Proc. Natl. Acad. Sci. U.S.A.* **104,** 2721–2726
4. Bigelow, R. L., Williams, B. J., Carroll, J. L., Daves, L. K., and Cardelli, J. A. (2009) *Breast Cancer Res. Treat.* **117,** 31–44
5. Schrohl, A. S., Holten-Andersen, M. N., Peters, H. A., Look, M. P., Meijer-van Gelder, M. E., Klijn, J. G., Brünner, N., and Foekens, J. A. (2004) *Clin. Cancer Res.* **10,** 2289–2298
6. Egeblad, M., and Werb, Z. (2002) *Nat. Rev. Cancer* **2,** 161–174
7. Itoh, Y., and Seiki, M. (2006) *J. Cell. Physiol.* **206,** 1–8
8. Yu, Q., and Stamenkovic, I. (1999) *Genes Dev.* **13,** 35–48
9. Yu, W. H., Woessner, J. F., Jr., McNeish, J. D., and Stamenkovic, I. (2002) *Genes Dev.* **16,** 307–323
10. Stamenkovic, I. (2000) *Semin. Cancer Biol.* **10,** 415–433
11. Ponta, H., Sherman, L., and Herrlich, P. A. (2003) *Nat. Rev. Mol. Cell Biol.* **4,** 33–45
12. Toole, B. P. (2009) *Clin. Cancer Res.* **15,** 7462–7468
13. Naor, D., Wallach-Dayan, S. B., Zahalka, M. A., and Sionov, R. V. (2008) *Semin. Cancer Biol.* **18,** 260–267
14. Orian-Rousseau, V. (2010) *Eur. J. Cancer* **46,** 1271–1277
15. de la Torre, M., Heldin, P., and Bergh, J. (1995) *Anticancer Res.* **15,** 2791–2795
16. Corte, M. D., González, L. O., Junquera, S., Bongera, M., Allende, M. T., and Vizoso, F. J. (2010) *J. Cancer Res. Clin. Oncol.* **136,** 745–750
17. Li, L., Heldin, C. H., and Heldin, P. (2006) *J. Biol. Chem.* **281,** 26512–26519
18. Orian-Rousseau, V., and Ponta, H. (2008) *Adv. Cancer Res.* **101,** 63–92
19. Bourguignon, L. Y. (2008) *Semin. Cancer Biol.* **18,** 251–259
20. Toole, B. P. (2001) *Semin. Cell Dev. Biol.* **12,** 79–87
21. de la Torre, M., Wells, A. F., Bergh, J., and Lindgren, A. (1993) *Hum. Pathol.* **24,** 1294–1297
22. Auvinen, P., Tammi, R., Parkkinen, J., Tammi, M., Agren, U., Johansson, R., Hirvikoski, P., Eskelinen, M., and Kosma, V. M. (2000) *Am. J. Pathol.* **156,** 529–536
23. Boregowda, R. K., Appaiah, H. N., Siddaiah, M., Kumarswamy, S. B., Sunila, S., Thimmaiah, K. N., Mortha, K., Toole, B., and Banerjee, S. (2006) *J. Carcinog.* **5,** 2
24. Camenisch, T. D., Spicer, A. P., Brehm-Gibson, T., Biesterfeldt, J., Augustine, M. L., Calabro, A., Jr., Kubalak, S., Klewer, S. E., and McDonald, J. A. (2000) *J. Clin. Invest.* **106,** 349–360
25. Li, Y., and Heldin, P. (2001) *Br. J. Cancer* **85,** 600–607
26. Zoltan-Jones, A., Huang, L., Ghatak, S., and Toole, B. P. (2003) *J. Biol. Chem.* **278,** 45801–45810
27. Jacobson, A., Rahmanian, M., Rubin, K., and Heldin, P. (2002) *Int. J. Cancer* **102,** 212–219
28. Koyama, H., Hibi, T., Isogai, Z., Yoneda, M., Fujimori, M., Amano, J., Kawakubo, M., Kannagi, R., Kimata, K., Taniguchi, S., and Itano, N. (2007) *Am. J. Pathol.* **170,** 1086–1099
29. Koyama, H., Kobayashi, N., Harada, M., Takeoka, M., Kawai, Y., Sano, K., Fujimori, M., Amano, J., Ohhashi, T., Kannagi, R., Kimata, K., Taniguchi, S., and Itano, N. (2008) *Am. J. Pathol.* **172,** 179–193
30. Udabage, L., Brownlee, G. R., Waltham, M., Blick, T., Walker, E. C., Heldin, P., Nilsson, S. K., Thompson, E. W., and Brown, T. J. (2005) *Cancer Res.* **65,** 6139–6150
31. Li, Y., Li, L., Brown, T. J., and Heldin, P. (2007) *Int. J. Cancer* **120,** 2557–2567
32. Suzuki, M., Asplund, T., Yamashita, H., Heldin, C. H., and Heldin, P. (1995) *Biochem. J.* **307,** 817–821
33. Jacobson, A., Brinck, J., Briskin, M. J., Spicer, A. P., and Heldin, P. (2000) *Biochem. J.* **348,** 29–35
34. Heldin, P. (2009) www.glycoforum.gr.jp/science/hyaluronan/HA33/HA33E.html
35. Zhang, W., Watson, C. E., Liu, C., Williams, K. J., and Werth, V. P. (2000) *Biochem. J.* **349,** 91–97
36. Jokela, T. A., Makkonen, K. M., Oikari, S., Kärnä, R., Koli, E., Hart, G. W., Tammi, R. H., Carlberg, C., and Tammi, M. I. (2011) *J. Biol. Chem.* **286,** 33632–33640
37. Jones, S., Jones, S., and Phillips, A. O. (2001) *Kidney Int.* **59,** 1739–1749
38. Wang, A., and Hascall, V. C. (2004) *J. Biol. Chem.* **279,** 10279–10285
39. Stern, R. (2008) *Semin. Cancer Biol.* **18,** 275–280
40. Heldin, P., de la Torre, M., Ytterberg, D., and Bergh, J. (1996) *Oncol. Rep.* **3,** 1011–1016
41. Deckers, M., van Dinther, M., Buijs, J., Que, I., Löwik, C., van der Pluijm, G., and ten Dijke, P. (2006) *Cancer Res.* **66,** 2202–2209
42. Heldin, P., and Pertoft, H. (1993) *Exp. Cell Res.* **208,** 422–429
43. Li, L., Asteriou, T., Bernert, B., Heldin, C. H., and Heldin, P. (2007) *Biochem. J.* **404,** 327–336
44. Persson, U., Souchelnytskyi, S., Franzén, P., Miyazono, K., ten Dijke, P., and Heldin, C. H. (1997) *J. Biol. Chem.* **272,** 21187–21194
45. Schmalfeldt, B., Prechtel, D., Härting, K., Späthe, K., Rutke, S., Konik, E., Fridman, R., Berger, U., Schmitt, M., Kuhn, W., and Lengyel, E. (2001) *Clin. Cancer Res.* **7,** 2396–2404
46. Itano, N., Zhuo, L., and Kimata, K. (2008) *Cancer Sci.* **99,** 1720–1725
47. Birkedal-Hansen, H., and Taylor, R. E. (1982) *Biochem. Biophys. Res. Commun.* **107,** 1173–1178
48. Akahane, T., Akahane, M., Shah, A., Connor, C. M., and Thorgeirsson, U. P. (2004) *Exp. Cell Res.* **301,** 158–167
49. Heldin, P., Laurent, T. C., and Heldin, C. H. (1989) *Biochem. J.* **258,**

919–922
50. Pienimaki, J. P., Rilla, K., Fulop, C., Sironen, R. K., Karvinen, S., Pasonen, S., Lammi, M. J., Tammi, R., Hascall, V. C., and Tammi, M. I. (2001) *J. Biol. Chem.* **276,** 20428–20435
51. Simpson, R. M., Wells, A., Thomas, D., Stephens, P., Steadman, R., and Phillips, A. (2010) *Am. J. Pathol.* **176,** 1215–1228
52. Vigetti, D., Rizzi, M., Viola, M., Karousou, E., Genasetti, A., Clerici, M., Bartolini, B., Hascall, V. C., De Luca, G., and Passi, A. (2009) *Glycobiology* **19,** 537–546
53. Pivetta, E., Scapolan, M., Wassermann, B., Steffan, A., Colombatti, A., and Spessotto, P. (2011) *J. Cell. Physiol.* **226,** 769–779
54. Schraufstatter, I., Serobyan, N., DiScipio, R., Feofanova, N., Orlovskaya, I., and Khaldoyanidi, S. K. (2009) *J. Stem Cells* **4,** 191–202
55. Ghatak, S., Misra, S., and Toole, B. P. (2005) *J. Biol. Chem.* **280,** 8875–8883
56. Karousou, E., Kamiryo, M., Skandalis, S. S., Ruusala, A., Asteriou, T., Passi, A., Yamashita, H., Hellman, U., Heldin, C. H., and Heldin, P. (2010) *J. Biol. Chem.* **285,** 23647–23654
57. Sato, N., Maehara, N., and Goggins, M. (2004) *Cancer Res.* **64,** 6950–6956
58. Olsson, M., Meadows, J. R., Truvé, K., Rosengren Pielberg, G., Puppo, F., Mauceli, E., Quilez, J., Tonomura, N., Zanna, G., Docampo, M. J., Bassols, A., Avery, A. C., Karlsson, E. K., Thomas, A., Kastner, D. L., Bongcam-Rudloff, E., Webster, M. T., Sanchez, A., Hedhammar, A., Remmers, E. F., Andersson, L., Ferrer, L., Tintle, L., and Lindblad-Toh, K. (2011) *PLoS Genet.* **7,** e1001332
59. Hibbard, M. K., Kozakewich, H. P., Dal Cin, P., Sciot, R., Tan, X., Xiao, S., and Fletcher, J. A. (2000) *Cancer Res.* **60,** 4869–4872
60. Unger, K., Wienberg, J., Riches, A., Hieber, L., Walch, A., Brown, A., O'Brien, P. C., Briscoe, C., Gray, L., Rodriguez, E., Jackl, G., Knijnenburg, J., Tallini, G., Ferguson-Smith, M., and Zitzelsberger, H. (2010) *Endocr. Relat. Cancer* **17,** 87–98
61. Tammi, R. H., Passi, A. G., Rilla, K., Karousou, E., Vigetti, D., Makkonen, K., and Tammi, M. I. (2011) *FEBS J.* **278,** 1419–1428
62. Lambert, E., Boudot, C., Kadri, Z., Soula-Rothhut, M., Sowa, M. L., Mayeux, P., Hornebeck, W., Haye, B., and Petitfrere, E. (2003) *Biochem. J.* **372,** 767–774
63. Liu, X. W., Bernardo, M. M., Fridman, R., and Kim, H. R. (2003) *J. Biol. Chem.* **278,** 40364–40372
64. Liu, X. W., Taube, M. E., Jung, K. K., Dong, Z., Lee, Y. J., Roshy, S., Sloane, B. F., Fridman, R., and Kim, H. R. (2005) *Cancer Res.* **65,** 898–906
65. Jung, K. K., Liu, X. W., Chirco, R., Fridman, R., and Kim, H. R. (2006) *EMBO J.* **25,** 3934–3942
66. Schlaepfer, D. D., and Mitra, S. K. (2004) *Curr. Opin. Genet. Dev.* **14,** 92–101
67. Liu, K. C., Huang, A. C., Wu, P. P., Lin, H. Y., Chueh, F. S., Yang, J. S., Lu, C. C., Chiang, J. H., Meng, M., and Chung, J. G. (2011) *Oncol. Rep.* **26,** 177–184
68. Paget, S. (1889) *Lancet* **1,** 571–573
69. Draffin, J. E., McFarlane, S., Hill, A., Johnston, P. G., and Waugh, D. J. (2004) *Cancer Res.* **64,** 5702–5711